Proc. Natl. Acad. Sci. USA
Vol. 95, pp. 14757–14762, December 1998
Cell Biology

Attachment to the nuclear matrix mediates specific alterations in chromatin structure

ALEXANDER PEMOV, SERGEI BAVYKIN*, AND JOYCE L. HAMLIN†

Department of Biochemistry and Molecular Genetics, University of Virginia School of Medicine, Charlottesville, VA 22908

Communicated by Oscar L. Miller, Jr., University of Virginia, Charlottesville, VA, October 9, 1998 (received for review August 16, 1998)

ABSTRACT **The DNA in eukaryotic chromosomes is organized into a series of loops that are permanently attached at their bases to the nuclear scaffold or matrix at sequences known as scaffold-attachment or matrix-attachment regions. At present, it is not clear what effect affixation to the nuclear matrix has on chromatin architecture in important regulatory regions such as origins of replication or the promoter regions of genes. In the present study, we have investigated cell-cycle-dependent changes in the chromatin structure of a well characterized replication initiation zone in the amplified dihydrofolate reductase domain of the methotrexate-resistant Chinese hamster ovary cell line CHOC 400. Replication can initiate at any of multiple potential sites scattered throughout the 55-kilobase intergenic region in this domain, with two subregions (termed *ori-β* and *ori-γ*) being somewhat preferred. We show here that the chromatin in the *ori-β* and *ori-γ* regions undergoes dramatic alterations in micrococcal nuclease hypersensitivity as cells cross the G_1/S boundary, but only in those copies of the amplicon that are affixed to the nuclear matrix. In contrast, the fine structure of chromatin in the promoter of the dihydrofolate reductase gene does not change detectably as a function of matrix attachment or cell-cycle position. We suggest that attachment of DNA to the nuclear matrix plays an important role in modulating chromatin architecture, and this could facilitate the activity of origins of replication.**

The DNA in eukaryotic chromosomes is periodically and permanently attached at specific sequences to a subnuclear scaffold or matrix to form a series of 30- to 100-kilobase (kb) loops (e.g., refs. 1–3; reviewed in refs. 4 and 5). Scaffold-attachment regions or matrix-attachment regions (MARs) (6, 7) are usually adenine/thymine-rich and, in many cases, contain consensus recognition sequences for topoisomerase II (8). Thus, it has been suggested that each chromosomal loop may constitute an independent domain of supercoiling (7). MARs have been shown to be favored sites for histone H1 binding *in vitro* and have been proposed to function as specific nucleation centers for H1-dependent chromatin repression (9, 10). It also has been suggested that MARs may facilitate the juxtaposition of important cis-regulatory sequences to their appropriate matrix-affixed replication, transcription, recombination, or processing machineries (reviewed in ref. 6). In the case of replication, evidence suggesting involvement of the matrix is substantial. For example, it has been shown that origins are situated close to the matrix during both initiation and chain elongation phases (11, 12), prompting the suggestion that origins correspond to permanently attached MARs (11–13). Additionally, many enzymes involved in replication are found in matrix preparations (reviewed in ref. 14), and there is considerable evidence that replication forks (11, 12, 15, 16), and possibly origins (17), are associated with the matrix. These findings have led to the suggestion that replication initiates at or near matrix-affixed origins and the remainder of each replicon is spooled through a matrix-associated replication complex (18, 19).

Our research has focused on identifying the cis- and trans-acting elements that regulate initiation of replication in mammalian chromosomes and determining how the activity of these elements is modulated by chromosome architecture. To study a single replicon type, we developed a methotrexate-resistant Chinese hamster ovary cell line (CHOC 400; ref. 20) that has amplified one of its dihydrofolate reductase (DHFR) genes and flanking sequences ≈1,000×. The 240-kb amplicons are maintained in stable, linear arrays at three different chromosomal locations (20). Two-dimensional (2-D) gel replicon mapping techniques have shown that nascent DNA strands can initiate at any of a large number of potential sites distributed throughout the 55-kb spacer region between the convergently transcribed DHFR and 2BE2121 genes (refs. 21 and 22; a map of the central 120 kb of the amplicon is shown in Fig. 1). However, more quantitative intrinsic labeling studies on early S-phase cells suggest that two subregions within the intergenic spacer are somewhat preferred (termed *ori-β* and *ori-γ*; refs. 23–28; also see refs. 29 and 30 for reviews). Several additional studies have focused on the *ori-β* region and have concluded that it constitutes the major initiation site in this locus (25–28). *Ori-β* and *ori-γ* lie ≈22 kb apart and, of interest, straddle a relatively prominent MAR (31). Recently, a novel homologous recombination strategy was used to delete the 4.3-kb fragment containing *ori-β* to determine whether it contains an essential genetic element (33). This deletion had no effect on either the timing or efficiency of initiation in the remainder of the initiation zone. Therefore, the loss of *ori-β* may be compensated for by redundant genetic elements in the neighborhood (e.g., *ori-γ*). Alternatively, origin activity may be regulated largely by chromosomal context, with only a minor contribution from sequences *per se*.

The *ori-β*/*ori-γ* locus is not a very efficient origin in CHOC 400 cells because initiation occurs in only 10–15% of amplicons in any given S period, with the remainder being replicated passively by forks from active origins in neighboring amplicons (22, 34); an interesting correlation is that only ≈15% of amplicons in CHOC 400 cells appear to be attached to the nuclear matrix at the intergenic MAR (31). In contrast, in parental Chinese hamster ovary cells with only two copies of the DHFR locus, a higher percentage of the origins fire and a correspondingly higher percentage of the DHFR domains are attached to the matrix at the intergenic MAR (31).

In the present study, we have asked whether attachment to the matrix correlates with alterations in chromatin architecture, specifically in the intergenic region and/or in the promoter of the DHFR gene. Our data show that the chromatin in the *ori-β* and *ori-γ* regions undergoes dramatic, cell-cycle-entrained alterations

The publication costs of this article were defrayed in part by page charge payment. This article must therefore be hereby marked "*advertisement*" in accordance with 18 U.S.C. §1734 solely to indicate this fact.

Abbreviations: kb, kilobase; MAR, matrix-attachment region; DHFR, dihydrofolate reductase; 2-D, two-dimensional; ORC, origin recognition complex.

*Present address: Center for Mechanistic Biology and Biotechnology, Argonne National Laboratory, Argonne, IL 60439.
†To whom reprint requests should be addressed. e-mail: jlh2d@virginia.edu.

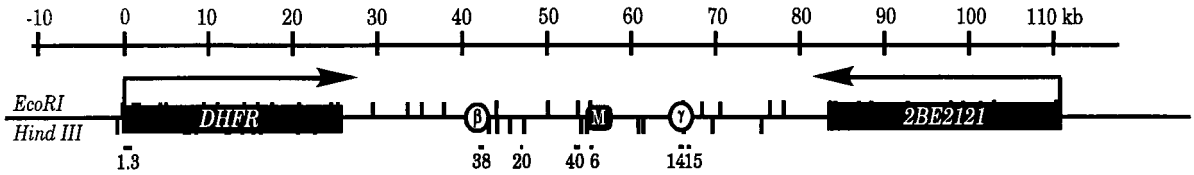

FIG. 1. Map of the Chinese hamster ovary DHFR initiation zone. The convergently transcribed DHFR and 2BE2121 genes are shown, as well as the two preferred initiation regions (*ori-β* and *ori-γ*) and the matrix attachment region (M) (31). *Eco*RI and *Hin*dIII sites are shown, and the approximate lengths and positions of the probes are indicated below the map (see *Materials and Methods* for details). The centers of the *ori-β* and *ori-γ* regions lie ≈1.2 and 0.25 kb in from the 3′ end of their respective *Hin*dIII fragments (23).

in micrococcal nuclease hypersensitivity but only in those copies of the amplicon that are affixed to the nuclear matrix.

MATERIALS AND METHODS

Cell Culture and Synchronization Protocols. CHOC 400 cells were maintained as monolayer cultures in minimal essential medium supplemented with nonessential amino acids and 10% HyClone II (termed MEM complete) and were maintained in an atmosphere of 5% CO_2/95% air. Cultures were harvested for nuclease studies in mid-log phase. Alternatively, they were synchronized by starving for isoleucine for 45 hr, which arrests them in G_0, followed by release into MEM complete containing 400 mM mimosine for 13 hr, which collects them at the G_1/S boundary (35). The drug then was removed and replaced with MEM complete medium, which allows relatively synchronous entry into the S period (35). All media and sera were obtained from GIBCO/BRL.

Micrococcal Nuclease Digestion Procedure. Micrococcal nuclease digestions were performed as described (36), with minor modifications. In brief, cells were lysed with 0.1% digitonin, and the nuclei were pelleted and washed once with cell wash buffer (5 mM Tris·HCl, pH 7.4/50 mM KCl/0.5 mM EDTA/0.05 mM spermine/0.125 mM spermidine/0.5% thiodiglycol/0.25 mM phenylmethylsulfonyl fluoride). Nuclei were resuspended in micrococcal nuclease digestion buffer containing 1 mM $CaCl_2$ at a concentration of 1.5 mg of DNA/ml and were subjected to partial digestion with 1.5 units of micrococcal nuclease (Worthington) per milligram of DNA in a total volume of 400 μl for 2–8 min at 37°C. Each preparation then was treated with 20 μg/ml pancreatic ribonuclease (Sigma) for 60 min at 37°, followed by 150 μg/ml Proteinase K (Amresco, Euclid, OH) for 120 min at 50°C, and DNA was purified by extraction with phenol/chloroform. Alternatively, digestion was performed on intact nuclei as above, and the histones then were extracted with the nonionic detergent lithium diiodosalicylate (6). The loop and matrix fractions were separated by centrifugation, with the matrix-attached DNA partitioning with the pellet. The control in all cases was naked DNA purified from asynchronous cultures of CHOC 400 cells.

Analysis of Micrococcal Nuclease Cutting Patterns by Indirect End Labeling (37). The resulting DNA preparations (along with the naked DNA control) were digested to completion with *Hin*dIII, were separated on a 1.4% agarose gel, and were transferred to Hybond N+ (Amersham). Digests were hybridized sequentially with the following probes (see *Results* and Fig. 1): probe 1.3, a 1.3-kb *Eco*RI fragment near the 5′ end of a 7.25-kb *Hin*dIII fragment containing the promoter; probe 38, a 0.4-kb fragment near the 3′ end of a 21-kb *Hin*dIII fragment containing *ori-β*; probe 14, a 1.7-kb fragment at the 3′ end of a 4.8-kb *Hin*dIII fragment containing *ori-γ*; probe 6, a 0.3-kb fragment near the 5′ end of a 6.1-kb *Hin*dIII fragment containing the MAR. In Figs. 2 and 5, the digests shown were from reactions that gave the clearest hypersensitive pattern in the DHFR promoter (which served as an internal control) (36).

The Neutral/Neutral 2-D Gel Replicon Mapping Technique (38). Cells were sampled at the times indicated in the legend to Fig. 4, and replication intermediates were prepared exactly as described (39). Replication intermediates were separated on a neutral/neutral 2-D gel by a modification (39) of the original protocol (38) and then were transferred to Hybond N+ and were hybridized with probe 38, which is specific for the 6.2-kb *Eco*RI fragment containing *ori-β*.

RESULTS

Micrococcal Nuclease Hypersensitive Sites Cannot Be Detected in the Intergenic Region in Total Chromatin Preparations from CHOC 400 Cells. In initial experiments, we examined the structure of *ori-β* and *ori-γ* by partial micrococcal nuclease digestion of total chromatin in nuclei isolated from asynchronous cultures (Fig. 2). This enzyme can detect distortions in the DNA backbone resulting from interactions with trans-acting factors and/or alterations in nucleosome spacing (see ref. 41 for review). Nuclei were isolated from actively dividing unsynchronized cells with digitonin and were digested partially with micrococcal nuclease to produce fragments 5–10 kb in length. As a control, naked DNA prepared from log cultures was digested similarly. After digestion to completion with *Hin*dIII, naked DNA (ND) and experimental samples (CHR) were separated on an agarose gel along with a size marker (M). The DNA in the gel then was transferred to a membrane and was analyzed by hybridizing with radioactive probes for the ends or near-ends of fragments of interest (37). This allows detection of any sites whose sensitivity to micrococcal nuclease is either enhanced or suppressed as a result of being packaged into chromatin (relevant probes and restriction fragments are indicated in Fig. 1 and are detailed in *Materials and Methods*). Several different film exposures were made to maximize detection of fragments in the higher and lower parts of each digest. Mid-range exposures are presented in Figs. 2 and 5. (Note that only the probe for *ori-γ* is a true end label; the ends of the probes for the promoter, *ori-β*, and the MAR lie ≈340, 525, and ≈500 bp from the local *Hin*dIII site, respectively. Thus, any hypersensitive sites lying in these intervals will not be detected by these probes, resulting in the absence of small fragments in the digests pictured in Figs. 2 and 5. True end labels devoid of repetitive elements could not be found for all of the relevant *Hin*dIII fragments, and other digests yielded unsuitable fragment distributions.)

In agreement with earlier studies (36, 42), the promoter region of the DHFR gene, which serves as an internal control in these experiments, is characterized by an irregular nucleosomal array and a number of hypersensitive and protected sites (arrowheads in left-hand panel of Fig. 2), most of which have been shown to correspond to transcription factor binding elements (43). A few additional differences can be detected in this experiment that are not observed reproducibly and therefore are not marked with arrows.

When this same digest was analyzed with a radioactive end label for *Hin*dIII fragments containing either *ori-β* (probe 38) or *ori-γ* (probe 14), no hypersensitive sites could be discerned; the only reproducible differences between the cutting patterns of naked DNA and chromatin were in the extent of protection of some sites (arrowheads in central two panels of Fig. 2; significance of open arrows is explained below). Hybridization of the membrane with an end label for the 6.1-kb fragment containing the MAR (probe 6) revealed several protected regions but no reproducible hypersensitive sites (Fig. 2 *MAR*, arrowheads). Successive hybridizations with additional probes (probes 20, 40, and

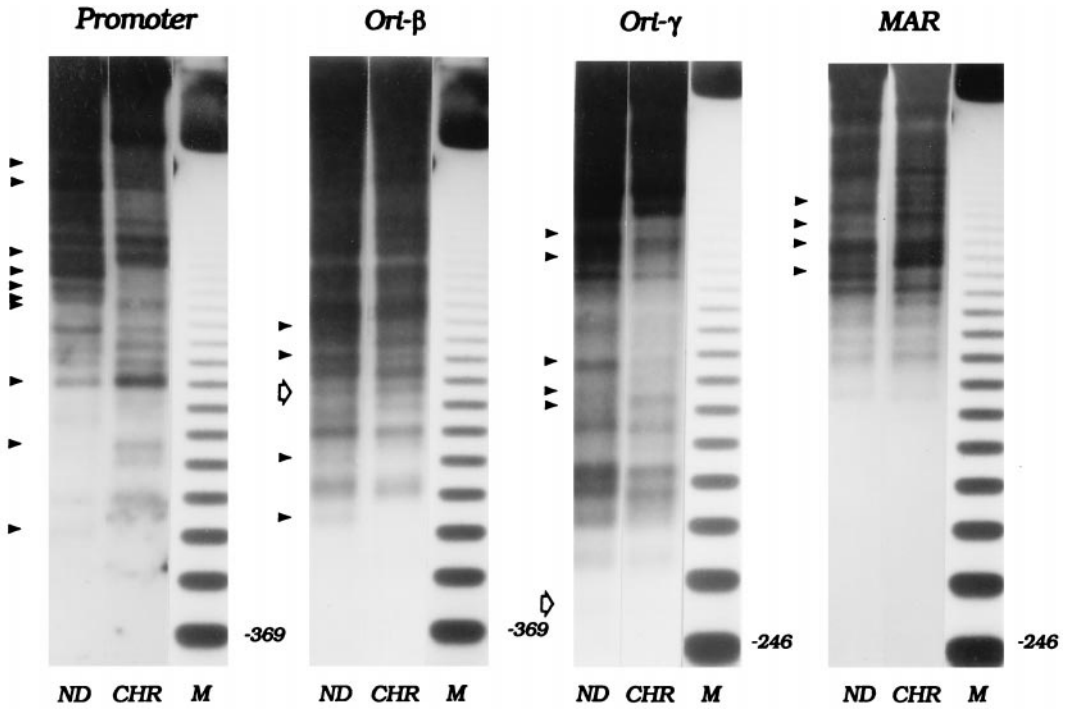

FIG. 2. Micrococcal nuclease digestion patterns of the DHFR domain in total chromatin from asynchronous CHOC 400 cells. Nuclei or naked DNA (ND) were isolated from an asynchronous culture of CHOC 400 cells and were subjected to partial micrococcal nuclease digestion as described in *Materials and Methods*. After digesting the DNA to completion with *Hin*dIII, the digests were separated on a 1.4% agarose gel and were transferred to Hybond N+. Digests were hybridized sequentially with probes for the indicated regions (see *Materials and Methods* and Fig. 1). ND, naked DNA; CHR, chromatin; M, 123-bp ladder. Solid arrowheads on the left side of each panel show the bands for which the kinetics of micrococcal nuclease digestion reproducibly differ between chromatin and naked DNA. Open arrows show the positions of cell-cycle-dependent hypersensitive sites that were detected in matrix-associated chromatin (see Fig. 5) but which are not detectable in the total chromatin samples studied in this experiment.

15; see Fig. 1) failed to illuminate any other gross and/or reproducible alterations in chromosome structure in other regions of the spacer (data not shown). In additional experiments on total chromatin from cells synchronized at the G_1/S boundary, in early S phase, or in G_2, we were also unable to detect any hypersensitive sites or other significant alterations in chromatin structure in the intergenic region, specifically, near the two origins or the MAR, even though the characteristic pattern of cutting in the DHFR promoter still was observed (data not shown).

The Pattern of Nuclease Hypersensitivity in the *ori-β* and *ori-γ* Regions Is Altered in a Cell-Cycle-Dependent Fashion, but Only in Matrix-Attached Chromatin. It was surprising that no obvious alterations in chromatin fine structure were detected in the *ori-β* and *ori-γ* regions, which are preferred regions for initiation in the DHFR domain in Chinese hamster ovary cells. However, only ≈15% of amplicons in CHOC 400 cells sustain active initiation events in any one cell cycle (22, 23), and we considered it possible that this fraction corresponds to the ≈15% that are attached to the nuclear matrix at the intergenic MAR (31). Therefore, only this small fraction might have an altered chromatin structure in the neighborhood of the origins, which could be masked by an undisturbed structure in the 85% of inactive amplicons.

To test this possibility, nuclei were isolated from an asynchronous culture of CHOC 400 cells by digitonin treatment and were digested lightly with micrococcal nuclease to illuminate hypersensitive sites. In this case, the micrococcal nuclease digestion simultaneously served to cleave matrix-proximal DNA from DNA situated farther out in the DNA loops (see Fig. 3). The nuclei then were treated with the nonionic detergent lithium diiodosalicylate to remove histones and other soluble nuclear proteins (6), and matrix-attached DNA was separated by centrifugation from the loop fraction (≈20 and 80% of total DNA, respectively). The two fractions were purified and digested to completion with *Hin*dIII, and fragments totaling ≈30 kb of DNA in the intergenic region were analyzed by indirect end labeling.

Although some differences were detected in the fine structure of the chromatin partitioning either with the matrix or loop fractions from unsynchronized cells, the differences were not reproducible, and no dramatic hypersensitive sites were detected in the intergenic spacer (A.P., unpublished work). Thus, although *ori-β* and *ori-γ* are the favored regions for initiation in the DHFR locus, no disturbances in the nucleosomal array could be detected. However, if hypersensitive sites at these locations are manifested during a relatively small window of the cell cycle, they could be masked in a sample of asynchronous cells. To examine this

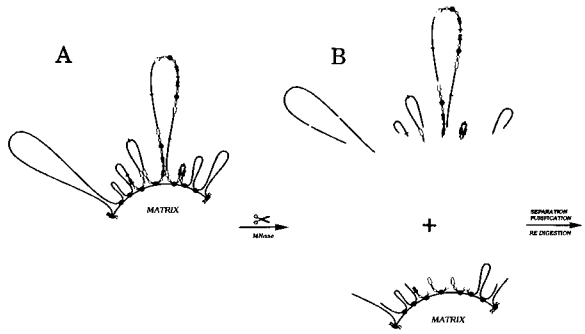

FIG. 3. Separating matrix-proximal DHFR amplicons from matrix-distal amplicons by partial micrococcal nuclease cleavage. (*A*) Organization of DHFR amplicons in CHOC 400 cells; all copies of the amplicon contain the intergenic MAR but only ≈15% of amplicons appear to be attached to the matrix at this site (31). Black arrows, DHFR genes; white arrows, 2BE2121 genes; filled circles, intergenic MARs; open circles, origins. (*B*) Micrococcal nuclease digestion was performed on intact nuclei so that subsequent manipulations to separate matrix-attached and loop fractions did not influence cut site distribution. DNA fragments from the matrix-affixed and loops fraction were purified, were digested with *Hin*dIII, and were electrophoresed on 1.4% agarose. After transfer to Hybond-N+, digests were hybridized with the probes indicated in *Materials and Methods* and *Results* and Fig. 1.

possibility, we analyzed the patterns of micrococcal nuclease hypersensitivity in synchronized cells. Cultures were released from a G_0 block into the replication inhibitor mimosine for 13 hr (time zero), at which point all cells reach the G_1/S boundary but initiation has not occurred in the intergenic region (35). After release from mimosine, the cells enter the S period in a synchronous wave, and 90 min later, initiation is maximal in the DHFR initiation zone (34, 35). This was confirmed by analysis of a fragment containing *ori-β* by the neutral/neutral 2-D gel replicon mapping approach (Fig. 4; ref. 38).

In this method, replication intermediates are isolated and digested to completion with an appropriate restriction enzyme. The digest is separated in a first-dimension gel on the basis of molecular mass (which, for any given replicating fragment, varies from 1*n* to just less than 2*n*, where 1*n* and 2*n* are unreplicated and completely replicated DNA, respectively) and in the second-dimension gel on the basis of both mass and shape. Branched replication intermediates containing either single forks (Fig. 4*A*), bubbles (Fig. 4*B*), or termination structures (not shown) migrate to characteristic positions in the gel, and intermediates in any fragment of interest can be analyzed by hybridization with an appropriate radioactive probe. When the 6.2-kb *Eco*RI fragment containing *ori-β* was detected with probe 38 in a sample blocked with mimosine, only the 1*n* spot corresponding to nonreplicating DNA was detected (Fig. 4*C*). However, 90 min after removal of mimosine, a prominent and characteristic 2-D gel pattern consisting of a bubble arc and a single fork arc was observed in the *ori-β*-containing fragment (Fig. 4*D*), as well as in all other fragments examined from the intergenic region (data not shown and refs. 21, 22, 34, and 35). This is the expected pattern for a fragment in a broad initiation zone because such a fragment will contribute to the bubble arc when initiations occur within the fragment itself but will contribute to the single fork arc when the fragment is replicated from an initiation site in a neighboring fragment in the initiation zone.

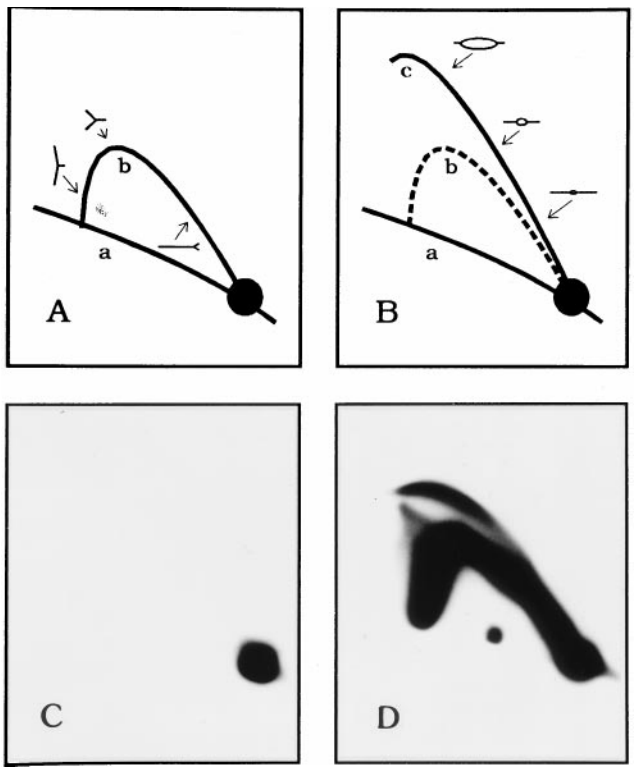

FIG. 4. Neutral/neutral 2-D gel analysis to confirm cell cycle position. (*A* and *B*) The 2-D gel replicon mapping method (38) separates a digest of replication intermediates in the first dimension according to molecular mass and in the second dimension according to both mass and shape. The nonreplicating restriction fragments in the genome trace a diagonal of linear fragments (curve a) whereas fragments containing single replication forks (*A*, curve b) or internal initiation sites (replication bubbles; *B*, curve c) are separated cleanly from the linear fragments and from each other. By hybridizing a transfer of such a gel with a probe specific for a fragment of interest, its mode of replication can be discerned. (*C*). 2-D gel analysis of a 6.2-kb *Eco*RI fragment containing *ori-β* in DNA isolated from cells blocked at the G_1/S boundary with mimosine (see *Materials and Methods*). No replication intermediates can be detected. (*D*) Analysis of the same *ori-β*-containing fragment 90 min after removal of mimosine, when initiation is at the peak in this locus.

Cells synchronized by this protocol were sampled at the G_1/S boundary 90 min after removal of mimosine or 13 hr later (representing a mixture of nonreplicating G_2, M, and early G_1 cells; data not shown), and the nuclei were subjected to partial cleavage with micrococcal nuclease as described above. As shown in Fig. 5, the pattern of micrococcal nuclease digestion of DNA in the promoter of the DHFR gene in both matrix and loop fractions is similar to that of total chromatin (compare with Fig. 2) and does not change detectably as a function of cell cycle position. In contrast, the patterns of nuclease digestion in the *ori-β* and *ori-γ* regions reveal important differences between the loop and matrix fractions: each region displays a pronounced hypersensitive site (open arrows), but only in the fraction that is attached to the nuclear matrix and only in chromatin from cells collected at the G_1/S boundary (labeled G_1 in Fig. 5). In the case of *ori-β*, the hypersensitive site lies ≈1,270 bp upstream from the right end of the 21-kb *Hin*dIII site detected with the probe 38 end label, very close to the adenine-rich tail of an *Alu*I-like element in this region of the intergenic spacer (44, 45). The site near *ori-γ* lies ≈270 bp upstream from the right end of the 4.8-kb *Hin*dIII fragment detected with probe 14 near a stretch of 15 adenines. Several other somewhat hypersensitive sites can be visualized in matrix-attached chromatin in the upper regions of the gel with the probe for the *ori-γ*-containing fragment. However, none of these appears to change as a function of the cell cycle.

Of importance, these micrococcal nuclease hypersensitive sites appear in cells that are arrested at the G_1/S boundary before initiation of nascent strands but not in samples taken 90 min after release from mimosine when initiation is maximal in this locus (Fig. 5, S90; refs. 21 and 22). In the 13-hr sample, which represents a mixture of G_2, mitotic, and early G_1 cells (labeled G_2 in the figure), the hypersensitive site in *ori-β* faintly reappears, but the site in *ori-γ* cannot be detected. As in total chromatin (Fig. 2), some minor differences between the naked DNA control and the chromatin fractions can be detected in the 6.1-kb *Hin*dIII fragment containing the MAR, and a few minor differences are evident between matrix and loop chromatin fractions. However, none of these change as a function of cell cycle position (Fig. 5).

DISCUSSION

We have examined chromatin in the intergenic region for micrococcal nuclease hypersensitive sites that might correspond to the presence of regulatory protein complexes or to other disturbances in chromatin structure that would render it more accessible to nuclease attack. The extent of reaction was adjusted to produce the characteristic pattern of hypersensitivity in the DHFR promoter, which served as an internal control. Digests were run for varying distances, and radioactive transfers were exposed to film for varying times to reveal as much of the spectrum of digestion products in each fragment as possible. Micrococcal nuclease/*Hin*dIII digests were examined with six different probes from the central 30-kb bracketing *ori-β*, *ori-γ*, and the MAR. Because our analysis probably would have detected a prominent hypersensitive site within 3–4 kb of the end of each probe, a total of ≈20 kb of DNA sequence was examined in this study. Only two prominent hypersensitive sites that varied with cell cycle position were detected, and these co-localize with the previously mapped *ori-β* and *ori-γ* regions (23–28). Of importance, these sites manifest themselves only in the matrix-attached fraction and, among the time points examined here, only at the G_1/S boundary. The sites are dissipated on entry into S-phase, apparently before initiation

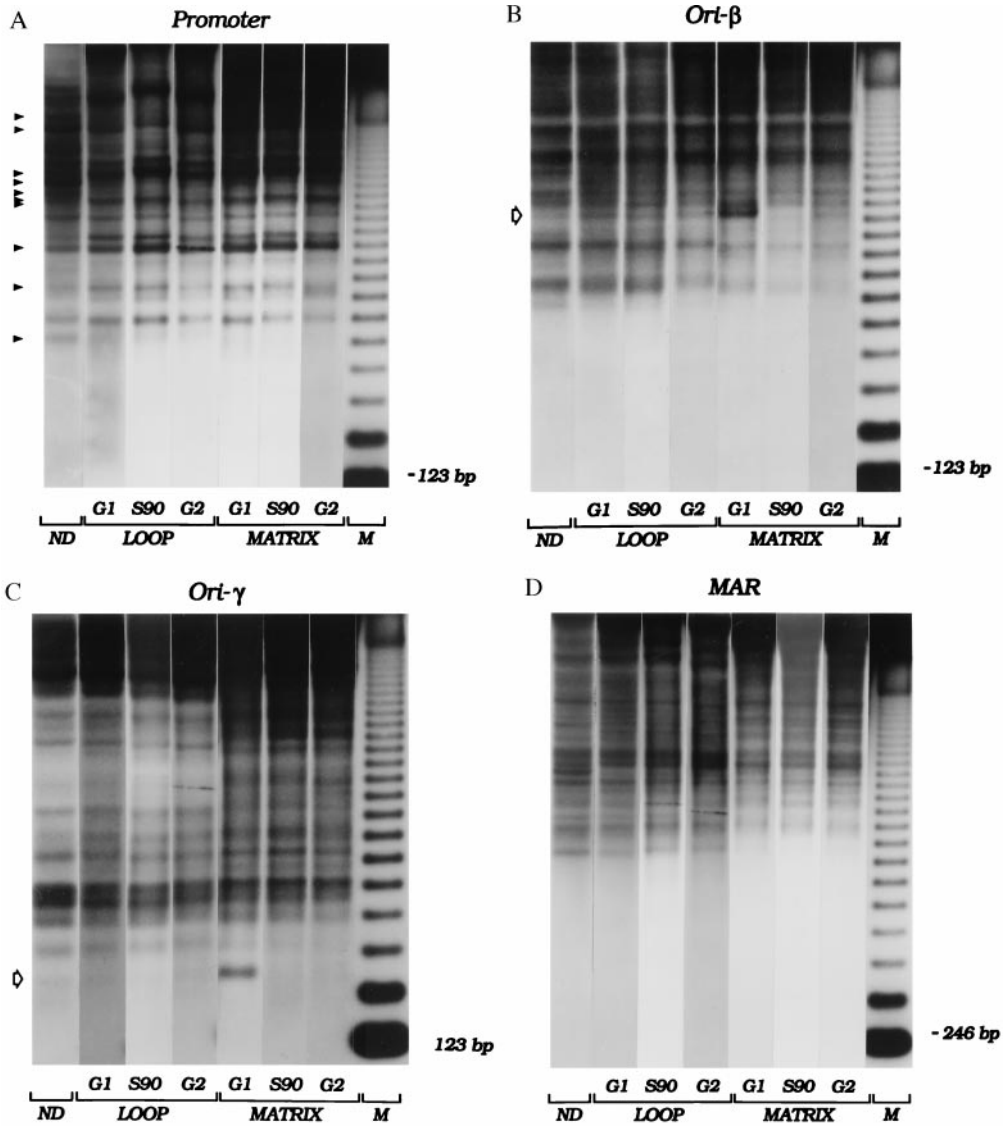

FIG. 5. Cell-cycle-dependent changes in chromatin architecture in matrix- associated and loop fractions. CHOC 400 cells were synchronized, and samples were taken before removal of mimosine (labeled "G_1 " in the figure), 90 min after drug removal ("S90" in the figure), or 13–14 hr after drug removal (representing a mixture of G_2, mitotic, and early G_1 cells; labeled "G_2 " in the figure). Isolated nuclei, in addition to a naked DNA control, were partially digested with micrococcal nuclease, and loop and matrix-associated DNA samples were purified, were digested with *Hin*dIII, and were separated on an agarose gel. After transfer to Hybond N+, the digests were hybridized sequentially with several end-labeled probes (see *Materials and Methods* and *Results* and Fig. 1). Panels labeled "Promoter", "*ori-β*", "*ori-γ*", and "MAR" are autoradiographs obtained with probes 1.3R1, 38, 14, and 6, respectively. Naked (ND), and loop- and matrix-associated DNA samples are indicated. M, 123-bp ladder. Open arrows on the left sides of the *ori-β* and *ori-γ* panels indicate prominent hypersensitive sites present only at the G_1/S boundary and only in matrix-associated chromatin.

at origins, because they cannot be detected in the peak initiation period 90 min after release from mimosine. Clearly, other hypersensitive sites also could be present that lie outside of the 20 kb of DNA sequence covered by this analysis.

The prominent cutting site in the *ori-β* region lies ≈600 bp upstream from a binding site for RIP60, a protein that was identified in gel-shift assays but whose function in replication initiation is presently unknown (46, 47). However, we have removed the 4.3-kb region bracketing *ori-β* (and the RIP60 binding site) from a cell line hemizygous for the DHFR locus, with no apparent effect on either the timing or efficiency of origin firing (33). Therefore, if *ori-β* is a critical genetic replicator, its function must be compensated for by an additional, redundant, element in the region. In this scenario, the interaction of a trans-acting factor with the replicators would be facilitated by local attachment to the nuclear matrix.

Alternatively, the hypersensitive sites at *ori-β* and *ori-γ* could correspond to DNA segments that are bared preferentially (or that assume a non-B-form structure) as a result of nearby attachment to the matrix. From preliminary genomic footprinting studies, we know that the *ori-β* hypersensitive site lies within an almost uninterrupted stretch of 55 adenines (corresponding to the polyA tail of an *Alu*I-like element in the region; refs. 44 and 45) whereas the site in *ori-γ* is near a stretch of 15 adenines. It is conceivable that a nearby attachment to the matrix promotes specific destabilization or distortion of the *ori-β* and *ori-γ* regions at these adenine/thymine-rich sites; when one or the other is removed, other sites might become the most accessible for loading of the replication complex. We presently are performing genomic footprinting to analyze detailed cutting patterns as a function of the cell cycle and as a function of the presence or absence of the *ori-β* region.

Cell-cycle-entrained disturbances in chromatin structure also have been detected in yeast replicators (48, 49). A prominent DNaseI hypersensitive site and a neighboring footprint are present over the autonomously replicating sequence *1* throughout the S and G_2 phases of the cell cycle, but as cells exit mitosis, the footprint expands and the hypersensitive site disappears (49). The footprint has been shown to result from occupancy by a specific origin recognition complex (ORC) (48, 50) and is extended, probably, by interaction of ORC with the Cdc6 gene product and a group of minichromosome maintenance proteins to form a prereplicative complex (51–54). After replication, the footprint contracts, and the hypersensitive site reappears (49). Because homologues to several of the ORC subunits now have been identified in several other species, including humans (reviewed in ref. 55), the important question regards whether the mammalian ORC complex recognizes specific sequences (replicators), as it does in *Saccharomyces cerevisiae*.

Although there is some evidence for the existence of genetic replicators in mammalian cells (56–58), in no case has a small required element been defined by the appropriate genetic strat-

egies that were used to discover and characterize yeast autonomously replicating sequence elements. For example, experiments designed to detect a replicator in the *ori-β* locus by testing its ability to support autonomous replication of a colinear sequence have been unsuccessful (ref. 59; P. K. Foreman, J. D. Milbrandt, and J.L.H., unpublished observations). However, several mammalian origins in addition to DHFR have been identified by mapping nascent strand start sites in regions of interest (see refs. 29 and 30 for reviews). In one of these (the human lamin B2 origin; refs. 60 and 61), cell-cycle modulations of chromatin structure also have been reported. The lamin B2 origin lies in the 500-bp region between the 3′ and 5′ ends of the lamin B2 gene and ppv1 genes, respectively (62). This origin was analyzed by dimethylsulfate and by partial DNaseI cleavage, and the products were analyzed on sequencing gels (60, 61). An invariant set of hypersensitive sites was detected, and a protected region ≈100 bp in length was observed in G_1 that shortened to ≈70 bp in S-phase and G_2. Thus, this pattern differs from the one reported here for the Chinese hamster DHFR initiation locus and from the pattern that characterizes yeast autonomously replicating sequence *1* (48, 49). The basis for these differences will not be understood fully until much more is known about the array of proteins that interact with each of these origins.

The clear association of the hypersensitive sites at *ori-β* and *ori-γ* only with matrix-associated chromatin provides compelling evidence that attachment to the matrix modulates chromatin configuration in at least one important class of regulatory regions (i.e., origins). It is possible that proximity of an origin region (Fig. 3*A*, closed circles) to a MAR could facilitate interaction of the origin with matrix-affixed regulatory protein complexes such as ORC merely by limiting the search volume of the interacting components. It might also be the case that ORC assembly requires the nuclear matrix to act as a scaffold, as suggested by the observation that prereplication foci, which form in G_1, partition with the nuclear matrix (63); the MAR then would correspond to the site at which the complex is loaded onto the DNA, followed by movement of the double helix through the complex to bring the origin into position for initiation.

A second possibility is that only a subset of potential MARs actually is attached to the matrix (as is the case for the intergenic MAR in the DHFR amplicons of CHOC 400 cells) and the distribution of attached sites is not even along the template. Thus, as shown in Fig. 3*A*, most amplicons will reside in large loops and only a fraction (15% in the case of CHOC 400 cells) would be amplicon-sized. If attachment to the matrix regulates torsional stress via topoisomerase II as has been suggested (7, 64), then perhaps only the smaller loops can attain the proper superhelical density (and therefore higher order chromatin structure) to facilitate origin recognition by initiator complexes. A third possibility (not pictured in Fig. 3*A*) is that origins may themselves be transiently affixed to the nuclear matrix before the time when they are activated, and this interaction would render them hypersensitive to nucleases. Although this association might also require attachment to the matrix at a nearby permanent MAR, this need not necessarily be the case. Deciding among these and other possibilities will be challenging. However, we believe that matrix association will prove to be critical for proper origin function and possibly for the functions of other important regulatory regions in DNA as well.

We are very grateful to Pieter Dijkwel, who performed the 2-D gel analysis presented in Fig. 4, as well as our technicians, Carlton White and Kevin Cox, for valuable technical support. We also thank all of the members of the Hamlin laboratory for lively and helpful discussions. This work was supported by Grant RO1 GM26108 from the National Institutes of Health.

1. Loc, P. V. & Stratling, W. H. (1988) *EMBO J.* **7,** 655–664.
2. Kellum, R. & Schedl, P. (1991) *Cell* **64,** 941–950.
3. Fishel, B. R., Sperry, A. O. & Garrard, W. T. (1993) *Proc. Natl. Acad. Sci. USA* **90,** 5623–5627.
4. Pienta, K. J., Getzenberg, R. H. & Coffey, D. S. (1991) *Crit. Rev. Eukaryotic Gene Expression* **1,** 355–385.
5. Dijkwel, P. A. & Hamlin, J. L. (1995) *Int. Rev. Cytol.* **162A,** 455–484.
6. Mirkovitch, J., Mirault, M. E. & Laemmli, U. K. (1984) *Cell* **39,** 223–232.
7. Cockerill, P. N. & Garrard, W. T. (1986) *Cell* **44,** 273–282.
8. Blasquez, V. C., Sperry, A. O., Cockerill, P. N. & Garrard, W. T. (1989) *Genome* **31,** 503–509.
9. Kas, E., Poljak, L., Adachi, Y. & Laemmli, U. K. (1993) *EMBO J.* **12,** 115–126.
10. Singh, L., Panicker, S. G., Nagaraj, R. & Majumdar, K. C. (1994) *Nucleic Acids Res.* **22,** 2289–2295.
11. Carri, M. T., Micheli, G., Graziano, E., Pace, T. & Buongiorno-Nardelli, M. (1986) *Exp. Cell Res.* **164,** 426–436.
12. Dijkwel, P. A., Wenink, P. W. & Poddighe, J. (1986) *Nucleic Acids Res.* **14,** 3241–3249.
13. Amati, B. & Gasser, S. M. (1990) *Mol. Cell. Biol.* **10,** 5442–5454.
14. Berezney, R., Mortillaro, M. J., Ma, H., Wei, X. & Samarabandu, J. (1995) *Int. Rev. Cytol.* **162A,** 1–65.
15. Vaughn, J. P., Dijkwel, P. A., Mullenders, L. H. & Hamlin, J. L. (1990) *Nucleic Acids Res.* **18,** 1965–1969.
16. Aelen, J. M., Opstelten, R. J. & Wanka, F. (1983) *Nucleic Acids Res.* **11,** 1181–1195.
17. Amati, B. B. & Gasser, S. M. (1988) *Cell* **54,** 967–978.
18. Pardoll, D. M., Vogelstein, B. & Coffey, D. S. (1980) *Cell* **19,** 527–536.
19. Dingman, C. W. (1974) *J. Theor. Biol.* **43,** 187–195.
20. Milbrandt, J. D., Heintz, N. H., White, W. C., Rothman, S. M. & Hamlin, J. L. (1981) *Proc. Natl. Acad. Sci. USA* **78,** 6043–6047.
21. Vaughn, J. P., Dijkwel, P. A. & Hamlin, J. L. (1990) *Cell* **61,** 1075–1087.
22. Dijkwel, P. A., Vaughn, J. P. & Hamlin, J. L. (1994) *Nucleic Acids Res.* **22,** 4989–4996.
23. Leu, T. H. & Hamlin, J. L. (1989) *Mol. Cell. Biol.* **9,** 523–531.
24. Anachkova, B. & Hamlin, J. L. (1989) *Mol. Cell. Biol.* **9,** 532–540.
25. Burhans, W. C., Selegue, J. E. & Heintz, N. H. (1986) *Proc. Natl. Acad. Sci. USA* **83,** 7790–7794.
26. Burhans, W. C., Vassilev, L. T., Caddle, M. S., Heintz, N. H. & DePamphilis, M. L. (1990) *Cell* **62,** 955–965.
27. Vassilev, L. T., Burhans, W. C. & DePamphilis, M. L. (1990) *Mol. Cell. Biol.* **10,** 4685–4689.
28. Pelizon, C., Diviacco, S., Falaschi, A. & Giacca, M. (1996) *Mol. Cell. Biol.* **16,** 5358–5364.
29. Hamlin, J. L., Mosca, P. J. & Levenson, V. V. (1994) *Biochim. Biophys. Acta* **1198,** 85–111.
30. DePamphilis, M. L. (1997) *Methods* **13,** 211–219.
31. Dijkwel, P. A. & Hamlin, J. L. (1988) *Mol. Cell. Biol.* **8,** 5398–5409.
32. Jacob, F. & Brenner, S. (1963) *C. R. Acad. Sci. Ser. III: Sci. Vie* **246,** 298–300.
33. Kalejta, R. F., Li, X., Mesner, L. D., Dijkwel, P. A., Lin, H.-B., and Hamlin, J. L. *Mol. Cell*, in press.
34. Dijkwel, P. A. & Hamlin, J. L. (1992) *Mol. Cell. Biol.* **12,** 3715–3722.
35. Mosca, P. J., Dijkwel, P. A. & Hamlin, J. L. (1992) *Mol. Cell. Biol.* **12,** 4375–4383.
36. Pemov, A., Bavykin, S. & Hamlin, J. L. (1995) *Biochemistry* **34,** 2381–2392.
37. Wu, C. (1980) *Nature (London)* **286,** 854–860.
38. Brewer, B. J. & Fangman, W. L. (1987) *Cell* **51,** 463–471.
39. Dijkwel, P. A., Vaughn, J. P. & Hamlin, J. L. (1991) *Mol. Cell. Biol.* **11,** 3850–3859.
40. Levine, A. J., Kang, H. S. & Billheimer, F. E. (1970) *J. Mol. Biol.* **50,** 549–568.
41. Elgin, S. C. (1990) *Curr. Opin. Cell Biol.* **2,** 437–445.
42. Azizkhan, J. C., Vaughn, J. P., Christy, R. J. & Hamlin, J. L. (1986) *Biochemistry* **25,** 6228–6236.
43. Azizkhan, J. C., Jensen, D. E., Pierce, A. J. & Wade, M. (1993) *Crit. Rev. Eukaryotic Gene Expression* **3,** 229–254.
44. Caddle, M. S., Lussier, R. H. & Heintz, N. H. (1990) *J. Mol. Biol.* **211,** 19–33.
45. Leu, T. H., Anachkova, B. & Hamlin, J. L. (1990) *Genomics* **7,** 428–433.
46. Dailey, L., Caddle, M. S., Heintz, N. & Heintz, N. H. (1990) *Mol. Cell. Biol.* **10,** 6225–6235.
47. Caddle, M. S., Dailey, L. & Heintz, N. H. (1990) *Mol. Cell. Biol.* **10,** 6236–6243.
48. Diffley, J. F. & Cocker, J. H. (1992) *Nature (London)* **357,** 169–172.
49. Diffley, J. F., Cocker, J. H., Dowell, S. J. & Rowley, A. (1994) *Cell* **78,** 303–316.
50. Bell, S. P. & Stillman, B. (1992) *Nature (London)* **357,** 128–134.
51. Cocker, J. H., Piatti, S., Santocanale, C., Nasmyth, K. & Diffley, J. F. X. (1996) *Nature (London)* **379,** 180–182.
52. Liang, C., Weinreich, M. & Stillman, B. (1995) *Cell* **81,** 667–676.
53. Aparicio, O. M., Weinstein, D. M. & Bell, S. P. (1997) *Cell* **91,** 59–69.
54. Tanaka, T., Knapp, D. & Nasmyth, K. (1997) *Cell* **90,** 649–660.
55. Rowles, A. & Blow, J. J. (1997) *Curr. Opin. Genet. Dev.* **7,** 152–157.
56. Kitsberg, D., Selig, S., Keshet, I. & Cedar, H. (1993) *Nature (London)* **366,** 588–590.
57. Frappier, L. & Zannis-Hadjopoulos, M. (1987) *Proc. Natl. Acad. Sci. USA* **84,** 6668–6672.
58. McWhinney, C. & Leffak, M. (1990) *Nucleic Acids Res.* **18,** 1233–1242.
59. Caddle, M. S. & Calos, M. P. (1992) *Nucleic Acids Res.* **20,** 5971–5978.
60. Dimitrova, D. S., Giacca, M., Demarchi, F., Biamonti, G., Riva, S. & Falaschi, A. (1996) *Proc. Natl. Acad. Sci. USA* **93,** 1498–1503.
61. Abdurashidova, G., Riva, S., Biamonti, G., Giacca, M. & Falaschi, A. (1998) *EMBO J.* **17,** 2961–2969.
62. Giacca, M., Zentilin, L., Norio, P., Diviacco, S., Dimitrova, D., Contreas, G., Biamonti, G., Perini, G., Weighardt, F., Riva, S., *et al.* (1994) *Proc. Natl. Acad. Sci. USA* **91,** 7119–7123.
63. Hozak, P., Hassan, A. B., Jackson, D. A. & Cook, P. R. (1993) *Cell* **73,** 361–373.
64. Gasser, S. M., Laroche, T., Falquet, J., Boy de la Tour, E. & Laemmli, U. K. (1986) *J. Mol. Biol.* **188,** 613–629.